Poly (Vinylidene Difluoride) Polymer in 1-Ethyl-3-methylimidazolium Acetate and Acetic Acid Containing Solvents: Tunable and Recoverable Solvent Media to Induce Crystalline Phase Transition and Porosity

G. Khokarale, S.; Jablonski, P; Nikjoo, Dariush; Dinh, VM; Sundman, Ola; Irgum, K; Mikkola, Jyri-Pekka

Published in:
Sustainable Chemistry

Published: 29/10/2022

sustainable chemistry

MDPI

Article

Poly (Vinylidene Difluoride) Polymer in 1-Ethyl-3-methylimidazolium Acetate and Acetic Acid Containing Solvents: Tunable and Recoverable Solvent Media to Induce Crystalline Phase Transition and Porosity

Santosh Govind Khokarale [1,*], Piotr Jablonski [1], Dariush Nikjoo [2], Van Minh Dinh [1], Ola Sundman [1], Knut Irgum [1] and Jyri-Pekka Mikkola [1,3,*]

[1] Technical Chemistry, Department of Chemistry, Chemical-Biological Centre, Umeå University, S-90187 Umeå, Sweden
[2] Division of Materials Science, Luleå University of Technology, S-97187 Luleå, Sweden
[3] Industrial Chemistry & Reaction Engineering, Department of Chemical Engineering, Johan Gadolin Process Chemistry Centre, Åbo Akademi University, FI-20500 Åbo-Turku, Finland
* Correspondence: santosh.khokarale@umu.se (S.G.K.); jyri-pekka.mikkola@umu.se (J.-P.M.)

Abstract: In this report, 1-ethyl-3-methylimidazolium acetate, [EMIM][AcO] ionic liquid (IL) and acetic acid (AA) comprised solvents were used for the thermal treatment of poly (vinylidene difluoride), PVDF. Here, besides the various combinations of IL and AA in solvents, the pure IL and AA were also applied as a solvent upon thermal treatments. The samples obtained after the treatment were analysed for structural and crystalline phase changes, porosity, and molecular weight distribution with various analytical techniques. The Kamlet-Taft parameters measurement of the IL and AA containing solvents with different solvatochromic dyes was also performed to examine their solvent properties and correlate with the properties of the treated PVDF materials. The treatment of PVDF with pure IL results in the formation of highly carbonaceous material due to extensive dehydrofluorination (DHF) as well as possibly successive cross-linking in the polymer chains. Upon IL and AA combined solvent treatment, the neat PVDF which composed of both α- and β crystalline phases was transformed to porous and β-phase rich material whereas in case of pure AA the non-porous and pure α-phase polymeric entity was obtained. A combined mixture of IL and AA resulted in a limited the DHF process and subsequent cross-linking in the polymer chains of PVDF allowed the formation of a porous material. It was observed that the porosity of the thermally treated materials was steadily decreasing with increase in the amount of AA in solvents composition and solvent with an AA:IL mole ratio of 2:1 resulted in a PVDF material with the highest porosity amongst the applied solvents. A recovery method for the IL and AA combined solvent after the thermal treatment of PVDF was also established. Hence, with varying the type of solvents in terms of composition, the highly carbonaceous materials as well as materials with different porosities as well as crystalline phases can be obtained. Most importantly here, we introduced new IL and AA containing recoverable solvents for the synthesis of porous PVDF material with the electroactive β-phase.

Keywords: poly (vinylidene difluoride); ionic liquid; acetic acid; crystalline phase transition; porosity; recoverable solvents

Citation: Khokarale, S.G.; Jablonski, P.; Nikjoo, D.; Dinh, V.M.; Sundman, O.; Irgum, K.; Mikkola, J.-P. Poly (Vinylidene Difluoride) Polymer in 1-Ethyl-3-methylimidazolium Acetate and Acetic Acid Containing Solvents: Tunable and Recoverable Solvent Media to Induce Crystalline Phase Transition and Porosity. *Sustain. Chem.* **2022**, *3*, 455–474. https://doi.org/10.3390/suschem3040028

Academic Editors: Ana B. Pereiro and João M. M. Araújo

Received: 22 September 2022
Accepted: 25 October 2022
Published: 29 October 2022

1. Introduction

Being electroactive due to its intrinsic piezoelectric as well as ferroelectric properties, poly (vinylidene fluoride), PVDF is the most industrially demanding fluorinated semi-crystalline polymer from last two decades. PVDF is widely used in electronic equipment, such as flexible piezoelectric sensors, energy storage devices, electroactive separator electrolyte in Li-ion batteries, etc. [1–5]. Besides electroactive properties, PVDF has good chemical resistance, high thermal stability, excellent mechanical strength, and an ability

to form membranes and therefore it is an important material for several industrial processes such as membranes for gas separation [6–8]. PVDF occurs generally in its three main multi-crystalline phases or polymorphs such as α, β, and γ among which, α-phase with TGTG′ (T-Trans and G-Gauche) conformation is electrically inactive. However, β and γ- phases with TTT and TTTGTTTG′ conformations, respectively, have electroactive properties [1,9,10]. However, when the G conformation is included in the molecular chain of γ-phase, it reduces the polarity significantly and influences the electrical properties. On the other hand, β phase shows the highest dipole moment per unit cell due to its special TT conformation and possesses superior energy harvesting ability compared to γ-phase.

The commercial PVDF which is obtained by crystallisation from the melt, contains dominant kinetically stable and non-polar α phase. Hence, to induce polarity and electroactive characteristics, it is necessary to perform the phase transformation towards β phase analogues and, in this regard, various methods have been developed. The methods such as mechanical stretching, annealing, high pressure exposure, electrospinning, and high-voltage electrostatic fields were applied and resulted to polar and electroactive polymer chains in PVDF [10]. Besides that, synthesis of composites through the addition of external additives such as metal oxides (ZnO, $BaTiO_3$, Nano clays), potassium bromide, molybdenum sulphide, graphene oxide, methylammonium lead iodide, precious metal nanoparticles (gold, silver, etc.), metal organic frameworks (MOFs), room temperature ionic liquids as well as carbon nanotubes are also used to induce the electroactive phases in PVDF [10–16]. In addition to enhancement of electroactive properties, additives also introduce hydrophilicity, porosity, and high ultraviolet resistance in PVDF, as well as improve its mechanical and anti-fouling properties.

Solvents based thermal processing was also extensively applied for the phase inversions or introduce polymorphism in PVDF where various types of dipolar aprotic solvents have been applied [9,17]. Previous studies revealed that the type of crystallisation phase forms after the dissolution as well as gelation of PVDF in solvent-based processing depends on the dipole moment of the solvent, hydrogen bonding ability and electrostatic interaction between polymer chains and solvent molecule as well as processing temperature [18,19]. During the dissolution, the solvent slowly diffuses or penetrate the PVDF polymeric chains and forms a swollen gel-like layer and further diffusion continue to form solvent-gel and gel-polymer like interfaces. The formation of these interfaces continues until complete dissolution of the polymer is achieved and to the formation of a single phase. The rate of this solvation process immensely depends on the polarity of the applied solvents where dipolar aprotic solvents due to their high polarizing ability efficiently solvates the polymer. Due to their high polarity, the polar solvents increase the rate of solvation process of polymer to the higher extent than in case of intermediate or less polar counterparts [20,21]. In previous reports, the Flory–Huggin's interaction parameter (χ_{12}) between PVDF and various solvents based on an inverse gas chromatography technique was applied to examine the extent of interaction between the polymer and solvent and its influence on the appearance of the crystalline phase during dissolution-gelation process [17,22]. It was observed that solvents with higher difference in the solubility parameters with PVDF ($\chi_{12} >> 0.5$) such as water, hexane, m-xylene, etc., are considered as non-solvents for dissolution of PVDF due to their poor solvation ability and were thus unable to introduce phase transition. The solvents like dimethyl sulfoxide (DMSO), dimethyl formamide (DMF), dimethyl acetamide (DMA), and n-methyl pyrrolidone (NMP) have χ_{12} values lower than 0.5 (high dipole moment) and possess stronger solvation ability with formation of a single solvent phase and, therefore, allow α to β phase transition. The ketones and lactones such as 3-heptanone, 3-hexanone, 3-pentanone, 3-octanone, cyclohexanone and gamma-valerolactone (GVL) have a χ_{12} value closer to 0.5 ($\chi_{12} \approx 0.5$). These types of solvents have lower to medium solvation ability (low to intermediate dipole moment) that allows the formation of thermoreversible gel after heating, followed by cool down the solution. GVL has the lowest χ_{12} value (higher solute-solvent interaction) compared to other ketone solvents, making it able to introduce γ-phase in the treated PVDF after gelation [22]. On the other hand, other above

mentioned ketone solvents with comparatively higher χ_{12} value, i.e., result in a weaker solvent-polymer interaction with PVDF in terms of α phase crystallinity.

The renewable solvents such as triacetin, cyrene™, ethylene and propylene carbonate, acetyl tributyl citrate, etc. also extensively applied for the processing of PVDF [23–26]. These solvents are considered as a sustainable alternative to toxic traditional solvents due to their greener and comparatively mild environmentally hazardous nature. Similar to traditional solvents, the renewable solvents also introduce the crystalline phase transitions in PVDF depending on their respective dipole moment strength and solvation ability. Supercritical fluids were also applied in dissolution of PVDF, where solvents such as dimethyl ether, supercritical CO_2 (with halogenated solvents), difluoromethane and acetone were used [27,28]. However, this study focused mainly on the dissolution whereas the changes in the crystalline phases were not adequately described. Hence, for the processing of PVDF and to induce electroactive phases various physical as well as solvents induced chemical methods have been applied. The solvent-based processing of PVDF is more preferred compared to physical treatment as well as introducing additives, since solvent-based methods provide a non-complicated and desired modifications in the polymer chains. In this regards, new solvent media are being periodically developed for PVDF treatment where solvents associated with their easy availability, cheapness, environment friendliness and possibly renewable characteristics are considered as the most preferable choices.

Ionic liquids (ILs) are a well-studied solvent media for the thermal processing of low to high molecular weight polymeric entities including synthetic as well as biopolymers [29–31]. Besides the high molecular weights, the intra- and intermolecular hydrogen bonding as well as cross-linking in the polymeric chains of polymer is the bottle neck of their dissolution and derivatization process. Since high temperature treatment with solvents facilitate the feasible processing of the polymers, the thermally stable solvents with high polarity are more demanding in this regard. ILs are known for their high thermal stability, highly polarity (since they are composed of ions in their structures), low vapour pressure as well as recyclability and, therefore, considered as suitable solvents for the processing of polymers. In this report, we describe the thermal processing of the PVDF in 1-ethyl-3-methylimidazolium acetate, [EMIM][AcO] ionic liquid (IL) and acetic acid (AA) embedded solvents. The crystalline phase change in the processed PVDF was confirmed by Fourier-transform infrared (FTIR), Raman and X-ray diffraction (XRD) spectroscopy techniques. The molecular weight distribution and porous characteristics of the treated PVDF were investigated by size exclusion chromatography (SEC) and N_2 physisorption analysis, respectively. Finally, the recovery method for the solvent comprised with IL and AA after the treatment of PVDF is also described.

2. Materials and Methods

2.1. Materials

The poly (vinylidene fluoride) (PVDF, Kynar® 740) pellet was obtained from Arkema whereas 1-ethyl-3-methylimidazolium acetate (97%), 4-Nitroaniline, Nile red dye (for microscopy), D_2O (99.9 atom% D) and DMSO-d^6 (99.96 atom% D) were purchased from Sigma Aldrich (St. Louis, MO, USA). N, N-diethyl-4-nitroaniline (98%) was purchased from Apollo Scientific. Acetic acid (glacial ≥99.7%) and acetone (≥99.5%) were purchased from VWR chemicals. All the chemicals and PVDF were used without further purification.

2.2. Methods

2.2.1. Synthesis of [EMIM][AcO] IL and Acetic Acid Containing Mixtures

The mixtures of [EMIM][AcO] IL and acetic acid (AA) were prepared to maintain AA:IL mole ratios of 0.5:1, 1:1, 2:1, 3:1, 4:1 and 6:1 in their compositions. The required amounts of IL and AA were mixed and stirred for 15 min at room temperature. The obtained mixtures were further stored at room temperature in desiccator prior to use for the treatment of PVDF and further analysis.

2.2.2. Differential Scanning Calorimetry (DSC) of [EMIM][AcO] IL and Acetic Acid Containing Mixtures

A Mettler DSC 821e differential scanning calorimeter (Mettler Toledo, Columbus, OH, USA) was used to measure the enthalpy changes associated with thermal transition of the mixtures. The desired amount of samples (5–10 mg) were sealed in ME-27331 aluminium crucibles with pierced lids and further subjected to a thermal treatment under nitrogen gas flow (80 mL/min). Initially, the samples were cooled down to −100 °C at a rate of −20 °C/min using liquid nitrogen and held under isothermal conditions for 5 min, and then heated at 10 °C/min from −100 to +100 °C.

2.2.3. NMR Analysis (Liquid State) of [EMIM][AcO] IL and Acetic Acid Containing Mixtures

The ^{1}H NMR spectra of the physical mixtures between IL and AA with mole ratios from 0.5:1, 1:1, 2:1, 3:1 as well as pure AA and IL were measured. Samples (≈25 mg) were dissolved in 0.5 mL DMSO-d^6 and analysis was carried with a Bruker (Billerica, MA, USA) DRX-400 spectrometer and data were further processed with the TopSpin 4.0.7 software from Bruker. The reaction mixtures obtained after the thermal treatment of PVDF in solvents such as pure IL and mixtures of IL and AA (AA:IL mole ratio = 1:1, 2:1 and 3:1) were measured upon ^{19}F NMR analysis. Approx. 50 mg of reaction mixtures were mixed with 1 mL of D_2O and stirred at room temperature for 15 min. The precipitated PVDF was allowed to settle at the bottom of the vial while 0.5 mL of supernatant solution was further used upon NMR analysis. The measurements as well as processing of the data was carried out similar to ^{1}H NMR analysis.

2.2.4. Kamlet-Taft Parameters Measurement of [EMIM][AcO] IL and Acetic Acid Containing Mixtures

Polarity characteristics of the pure IL and AA as well as mixtures obtained after their combinations were evaluated in terms of Kamlet-Taft or solvatochromic parameters such as hydrogen bond acidity (α), hydrogen bond basicity (β) and dipolarity or polarizability (π*). Initially, the solution of Nile red dye (0.042 mM) in acetone and 0.1 mM solution of 4-nitroaniline and N, N-diethyl-4-nitroaniline in methanol were prepared. Subsequently, 100 µL of Nile red dye (NR) solution or 25 µL solution of 4-nitroaniline (4NA) or N, N-diethyl-4-nitroaniline (D4NA) solution was transferred into a 5 mL glass vial and dried under nitrogen gas flow. Further, 1 g of IL, AA or mixed solvents were added to a vial containing dye and dissolved at 25 °C by sonication. The absorption spectra of mixtures of dye and solvents was measured on a Mettler Toledo UV5Bio UV–Vis spectrophotometer (300–800 nm) using a quartz cuvette. The Kamlet-Taft parameters were calculated by Equations (1)–(4), respectively.

$$\upsilon_{(\text{D4NA or 4NA or NR})} = \frac{1.035(\upsilon_{\text{D4NA}} + 2.64 - \upsilon_{\text{4NA}})}{\lambda_{\text{max, D4NA or 4NA or NR}} \times 10^{-4}} \quad (1)$$

$$\pi^* = 0.314\,(27.52 - \upsilon_{4DNA}) \quad (2)$$

$$\beta = \frac{1.035(\upsilon_{\text{D4NA}} + 2.64 - \upsilon_{\text{4NA}})}{2.80} \quad (3)$$

$$\alpha = \frac{(19.9657 - 1.0241\pi^* - \upsilon_{\text{NR}})}{1.6078} \quad (4)$$

where, $\lambda_{max,D4NA}$, or $\lambda_{max,4NA}$, or $\lambda_{max,NR}$, correspond to the maximum absorption wavelength of N, N-diethyl-4-nitroaniline, 4-nitroaniline and Nile Red, respectively.

2.2.5. Thermal Treatment of PVDF in [EMIM][AcO] IL and Acetic Acid Containing Mixtures

Pure IL and AA as well as their mixtures with various AA:IL mole ratios were used as a solvent for thermal processing of PVDF. In this case, 2 g of the reaction mixture comprising

of 10 wt.% PVDF pellets in various solvents were stirred at 140 °C for 1 h in 5 mL screw-cap glass vials in a preheated aluminium metal block. The treated reaction mixtures were cooled down to room temperature and further mixed with 50 mL of distilled water under vigorous stirring to precipitate out the PVDF material. The solid material was recovered using vacuum filtration technique and washed with fresh distilled water (4 × 25 mL). The materials were freeze dried overnight and obtained solid was stored in desiccator prior to the analysis.

2.2.6. Analysis of PVDF after Treatment with Various Solvents

The ^{13}C CP/MAS NMR analysis of neat and regenerated PVDF was carried out by Bruker 500 MHz Avance III instrument and TopSpin 4.0.7 software from Bruker was used for the data processing. The crystallinity of neat PVDF and regenerated PVDF was confirmed by powder XRD on PANalytical instrument in a diffraction intensity range of 2θ = 10–70°, at a scanning rate of 10°/min. Dispersive Raman spectra were recorded on a Renishaw Qontor instrument (Renishaw Plc, Wotton-under-Edge, UK), using a 532 nm laser with a maximum laser power of 50 mW, operating at 0.1–50% total power. Exposure time was 1 s for all samples, and 10 scans were co-added. A 20 × lens was used, and spectra were recorded in normal confocal settings in static mode, centred at 1200 cm^{-1}. The Attenuated Total Reflectance-Fourier Transform Infrared Spectroscopy (ATR-FTIR) technique was used in the analysis of the functional groups of neat and regenerated PVDF by a Bruker Vertex 80v FT-IR spectrometer (vacuum bench) with DTGS detector. The molecular weight distributions (MWDs) of the neat as well as thermally treated PVDF in various solvents were analysed by using Size Exclusion Chromatography (SEC). In this case, the SEC instrument was coupled with Multi-Angle Light Scattering (MALS) detector which working at 14 angles between 36 and 140° in DMAc as the solvent. Besides that, the SEC system consisted of a guard column and two serial T6000M columns from Malvern. The temperatures were set at 50 °C, and the flow rate was 1 mL/min. The detector system consisted of a refractive index and MALS detector where two pullulan standards (PSS) were used to calibrate the detectors. The obtained data were processed by using a Debye model in the OMNISEC V11 software from Malvern.

2.2.7. Recovery of [EMIM][AcO] IL and Acetic Acid Mixture (AA:IL Mole Ratio of 3)

The reaction mixture with 10 wt.% of dissolved PVDF in solvent with a AA:IL mole ratio 3 was used for the recovery of the solvent from treated PVDF. In this case, 2 g of the total reaction mixture was mixed with 25 mL of acetone and stirred for 30 min. The precipitated PVDF was separated by filtration and washed 3 times (10 mL each time) with fresh acetone. The IL and AA was further recovered by evaporation of acetone using rotation evaporator. The percentage recovery and purity of the recovered IL and AA mixture was confirmed by Equation (5) and NMR analysis (in D_2O), respectively.

$$\% \text{ recovery} = \frac{(\text{Amount of IL and AA mixture recovered})}{(\text{Amount of IL and AA mixture used})} \times 100 \quad (5)$$

3. Results

3.1. Differential Scanning Calorimetry (DSC) of [EMIM][AcO] IL and Acetic Acid Mixtures

Figure 1 shows the DSC curves for the pure [EMIM][AcO] IL and acetic acid (AA) as well as their physical mixtures with AA:IL mole ratios of 2:1, 3:1 and 4:1, respectively. The neat [EMIM][AcO] IL shows a glass transition temperature (T_g) of −72 °C [32]. Besides that, pure AA also shows sharp and intense signal for its melting temperature at 14 °C. For mixtures of IL and AA, the T_g values were decreased steadily, whereas the intense characteristic signal for the melting temperature of AA disappeared. The T_g value for the mixture of AA:IL mole ratios of 1:1, 2:1 and 3:1 decreased to −89.8, −95.3 °C and −97.2 °C, respectively. The value with the mole ratio 4:1 was not observed since DSC analysis was measured until −100 °C. Our previous study regarding the DSC analysis of

[EMIM][AcO] IL and crotonic acid comprised mixtures also provided similar observation where the T_g values for the IL and acid mixtures were decreased as acid amount increased in the composition [33]. The mixtures obtained from IL and AA are the combination of hydrogen bond acceptor (HBA) and hydrogen bond donor (HBD) and have the ability to form deep eutectic solvents (DESs) through hydrogen bonding interactions [34]. Since DSC analysis shows glass transition temperatures instead of distinct melting points, the hydrogen bonding interaction between IL and AA indicates that low temperature transition mixtures (LTTMs) are formed, instead of DESs [35].

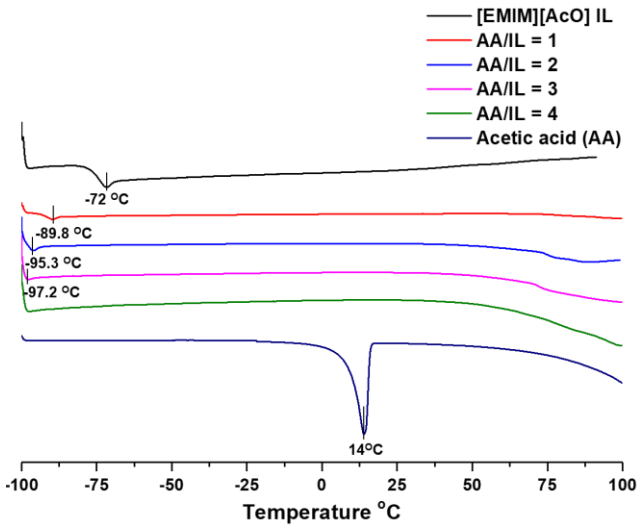

Figure 1. DSC study of the pure [EMIM][AcO] IL and acetic acid (AA) and their mixtures with varying AA/IL molar ratios 1:1, 2:1, 3:1 and 4:1.

3.2. ^{1}H NMR Analysis of [EMIM][AcO] IL and Acetic Acid Mixtures

The ^{1}H NMR analysis of the IL and AA containing mixtures was carried out and obtained spectra are shown in Figure 2b. Similar to our previous reports regarding interactions between IL and crotonic acid, changes in the chemicals shifts of protons of both AA and IL were also observed in the ^{1}H NMR spectra of the mixtures of IL and AA [33]. The chemical shift of the C2 proton of the imidazolium cation decreased with an increase in the AA:IL ratio. In addition, the distance between the signals of the C4 and C5 also decreased with an increased amount of AA. In case of AA, the de-shielding of the acidic proton in the -COOH group occurred compared to pure acid due to its possible ionic interaction with AcO^- anion in the IL (Figure 2a,b). These changes in the chemical environment of the protons in both AA and IL are the result of the hydrogen bonding interactions between AA and AcO^- anion of the IL. As described previously, similar interactions allowed the formation of eutectics or LTTMs between AA and IL (Figure 1).

3.3. Kamlet-Taft Measurements of [EMIM][AcO] IL and Acetic Acid Mixtures

The solvent properties such as dipolarity and hydrogen bonding ability of the IL and AA containing mixtures were investigated by calculating Kamlet-Taft parameters. The Kamlet-Taft parameters such as α, β and π* were quantified for their hydrogen bond donating ability (acidity), hydrogen bond accepting ability (basicity) and dipolarity or polarizability, respectively, in the applied solvents and the results obtained are displayed in Table 1. Besides that, the difference between the hydrogen bonding basicity and acidity (β-α), i.e., the net-basicity parameter was also calculated, which further provides more information about the overall basicity of the applied mixtures than considering β parameter alone.

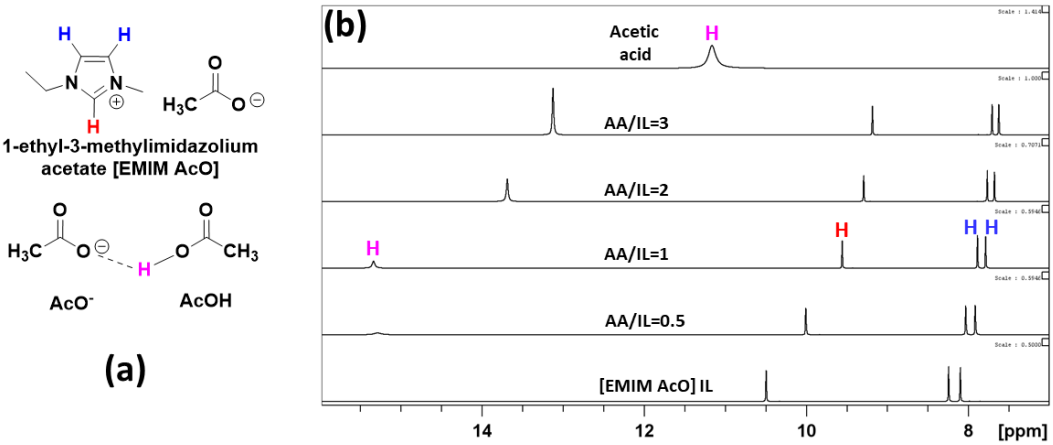

Figure 2. (**a**) Structure of [EMIM][AcO] IL and possible interaction between AcO^- anion and acetic acid, and (**b**) ^1H NMR spectra of the mixtures of IL and AA with varying ratios 0.5:1, 1:1, 2:1, and 3:1.

Table 1. Kamlet-Taft parameters obtained for the applied solvents for the treatment of PVDF.

Solvent	α	β	π*	β-α
[EMIM][AcO] IL	0.41	1.03	1.08	0.62
AA/IL = 1	0.45	0.85	1.01	0.40
AA/IL = 2	0.47	0.65	0.98	0.17
AA/IL = 3	0.57	0.56	0.97	−0.01
AA/IL = 4	0.64	0.49	0.94	−0.15
AA/IL = 6	0.84	0.47	0.91	−0.37
Pure AA	0.91	0.41	0.65	−0.50

The Kamlet-Taft parameters for [EMIM][AcO] IL in previous reports were evaluated by commonly used Reichardt's dye (Betaine 30) [36,37]. Since the mixtures of IL and AA as well as pure AA in the present study are acidic, the Reichardt's dye is not compatible to measure the Kamlet-Taft parameters. However, the parameters obtained for pure IL by introducing Nile red dye during measurements are identical to the previous reports where Reichardt's dye was applied [38]. As shown in Table 1, pure IL represents a β-α value of 0.6 and it is highest amongst the applied solvents considering its intrinsic basicity. For mixtures with an AA:IL mole ratio of 1:1, 2:1, 3:1, 4:1 and 6:1, the net basicity parameter's (β-α) value was progressively decreasing and turned to negative for higher AA:IL mole ratios since the AA concentration increased in the compositions of mixtures. The value of π* parameter was not significantly influenced with the AA amount when compared with pure IL and, until an AA:IL mole ratio of 6:1 and remained above the 0.9. This shows that the polarizing ability of the prepared mixtures of IL and AA have retained identical to pure IL. Pure AA showed further reduction in the net-basicity when compared to mixtures with IL and decreased to −0.5. Besides that, the polarizing ability of AA was also reduced, and it decreased to 0.65. Polarity parameters measurements demonstrate that IL and its mixtures with AA possess variable basic characteristics with high polarity and has the ability to establish powerful solvent-solute interactions to solubilize the embedded solute incorporated.

3.4. Thermal Processing and Recovery of PVDF in [EMIM][AcO] IL and Acetic acid Containing Mixtures

The 10 wt.% of PVDF amount was thermally treated at 140 °C for 1 h in pure [EMIM][AcO] IL and AA as well as their mixtures having AA:IL mole ratios from 1:1, 2:1, 3:1, 4:1 and 6:1. As shown in Figure 3A, considering the physical appearances of the reaction mixtures after the thermal treatment, the applied solvents including pure IL and AA were allowed either dissolution and/or decolouration of the PVDF. Black coloured

solid particles were obtained after interaction of PVDF material with pure IL while comparatively big size black coloured solid particles suspended in black-brown viscous liquid were observed after the treatment of PVDF in solvent with AA:IL mole ratio of 1:1. In case of solvent with an AA:IL mole ratio of 2:1, highly viscous, transparent, and dark brown coloured viscous liquid was obtained. The transparent and viscous liquids were observed with remaining reaction mixtures when solvents with AA/IL mole ratios 3:1, 4:1 or 6:1 were used. The haziness in the reaction mixtures was observed after keeping them for overnight where solvents with AA:IL mole ratio of 6:1 was used. With pure AA, the reaction mixture was transparent and colourless at reaction temperature whereas non-transparent and viscous liquid was observed after cooling down (Figure 3A(g)). Hence, the reaction mixtures gave rise to different physical appearances after thermal treatment depend on type of solvent media applied.

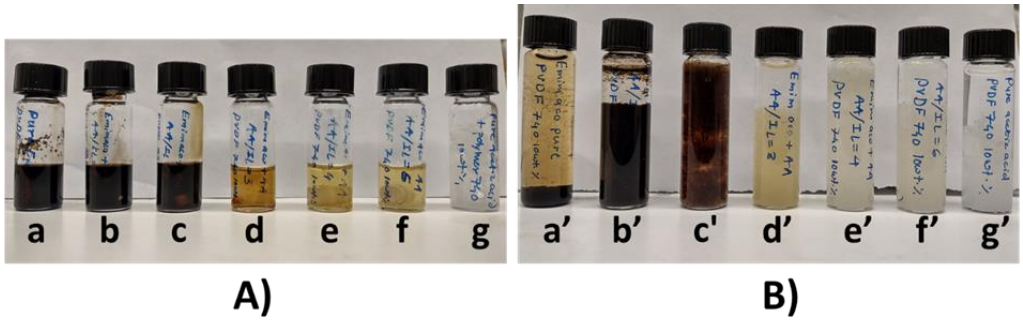

Figure 3. (**A**) Reaction mixtures after the thermal treatment of PVDF with (a) pure [EMIM][AcO] IL, IL and AA mixtures with AA/IL mole ratio (**b**) 1:1, (**c**) 2:1, (**d**) 3:1, (**e**) 4:, (**f**) 6: and (**g**) pure acetic acid (AA). Amount of PVDF = 10 wt.%, Temperature = 140 °C, Time = 1 h; (**B**) Addition of water in the thermally treated PVDF and various solvents containing reaction mixtures.

After addition of water in obtained reaction mixtures, the solid material was precipitated and separated since PVDF is not soluble in aqueous medium (Figure 3B). The dense and black coloured fine particles were settled at the bottom in pure IL comprised reaction mixtures (Figure 3B(a')). For solvent with an AA:IL mole ratio of 1:1, a fraction of black coloured solid material settled at the bottom of the vial and remaining material was swelled in water (Figure 3B(b')). In this case, rather than fine black particles, clusters of black solids appeared at the bottom of reaction vial. For reaction mixtures with solvents comprised of AA:IL mole ratios of 2:1, 3:1, 4:1 and 6:1 as well as pure AA, the dissolved material precipitated and remained swelled in aqueous medium (Figure 3B(c'–g')).

The recovered materials obtained after the separation from reaction mixture showed different appearances depending on type of solvent system applied during thermal treatment (Figure 4). Upon use of pure IL, fine black coloured solid material was obtained whereas black coloured solid particles similar to the size of neat PVDF were obtained after treatment of PVDF in solvent with AA:IL mole ratio of 1:1. After cutting these particles to small pieces, the unreacted, white coloured PVDF was observed inside. Further, the cotton like solid materials with variable colours were observed in case of solvents with AA:IL mole ratios of 2:1, 3:1, 4:1 and 6:1, as well as pure AA. The brown coloured solid was obtained after treating PVDF in a solvent mix containing AA:IL mole ratio of 2:1, while the white creamy coloured solids were obtained when solvents with AA:IL mole ratios of 3:1, 4:1 and 6:1 were used. The white coloured solid was obtained after treating PVDF in pure AA.

Figure 4. Recovered materials after treatment of in PVDF in [EMIM][AcO] IL, AA and DESs with varying AA:IL mole ratios, (**a**) neat PVDF, thermally treated PVDF in (**b**) pure IL, (**c**) AA:IL = 1:1, (**d**) AA:IL = 2:1, (**e**) AA:IL = 3:1, (**f**) AA:IL = 4:1, (**g**) AA:IL = 6:1 and, (**h**) pure AA. Temperature = 140 °C, time = 1 h.

The Kamlet-Taft parameter study represents that the pure IL possesses high basicity as well as polarity and, therefore, it possesses the dissolution capacity as well as simultaneous degradation of PVDF by inducing extensive dehydrofluorination (DHF). As a consequence, through the loss of hydrogen fluoride (HF), black coloured and highly carbonaceous material is formed (Figure 5) [39]. In case of solvent with AA:IL mole ratio of 1:1 (even though it has enough neat basicity a well as polarizing ability) the dissolution as well as DHF of PVDF did not properly occur. Here, an equivalent interaction between the IL and AA probably suppresses individual components interaction with the PVDF polymeric chains. The solvents with AA:IL mole ratios of 2:1, 3:1, 4:1 and 6:1 allowed complete dissolution of PVDF to form single phase as these solvents are combined with high polarizing ability (Table 1). As described previously, the molecular but neutral solvents such as DMSO, DMF, DMA, NMP possess π^* values close to value of 1 and are able to efficiently dissolve PVDF to the formation of a single phase [19,21]. Since the solvent mix with AA:IL mole ratio 2:1 has a lower, but positive net basicity value, the DHF of PVDF probably occurred in a small extend and hence, the brown coloured material was obtained after thermal treatment. However, due to negligible or absence of basic characteristics, the solvents with mole ratios of 3:1, 4:1 and 6:1 were only allowed the dissolution the PVDF. In case of pure AA, even though the π^* value decreased to 0.65, it was possible to dissolve the polymer at high temperature. However, due to lower polarizing ability compared to solvents obtained after its mixture with IL, the dissolved polymer was further precipitated in the form of a non-transparent gel, at room temperature. Hence, applied solvents containing IL and AA for the thermal treatment of PVDF allowed various solute-solvent interactions which was governed by their composition dependent properties such as basicity as well as polarizing ability.

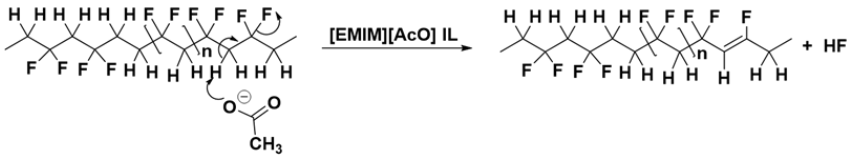

Figure 5. Dehydroflurination of PVDF in [EMIM][AcO] IL through release of HF.

3.5. ^{19}F NMR Analysis of Reaction Mixtures Obtained after Thermal Treatment of PVDF in Various Solvents

To confirm the DHF in the polymeric chains of PVDF in pure IL as well as other solvents comprised of IL and AA mixtures, the reaction mixtures obtained after the thermal treatment were further analysed by ^{19}F NMR. As shown in Figure 6, the intense peak for the F atom can be observed at −123.2 ppm for the reaction mixture when the pure IL was applied. It shows that IL degraded the PVDF through DHF process under thermal

treatment and released HF in the reaction mixture, thus carbonizing the PVDF to a carbon-rich material (Figures 4 and 5). The ^{19}F NMR spectra of the reaction mixtures with solvents containing AA:IL mole ratio of 1:1 also gave rise to a peak for the F atom; however, the intensity was lower by compared to the pure IL involving reaction mixture. Hence, the solvent mix with an equivalent mixture of IL and AA also allowed DHF of PVDF but to a smaller extent as AA decreases the basicity of the IL through acid-base neutralization. In this case, even though the solvent mix contains an equivalent mixture of IL and AA, at high temperature this induces availability of the acetate anion obtained after the neutralization and, therefore allows DHF of PVDF (Figure 2a). Similar observation was observed in our previous report since even though excess equivalent of crotonic acid formed after depolymerisation of poly (3-hydroxybutyrate), it did not significantly influence the rate of IL catalysed depolymerisation to a certain extend [33]. The peak intensity in case of reaction mixture comprised of solvent with an AA:IL mole ratio of 2:1 was significantly lower compared to the case with reaction mixtures containing pure IL and its equivalent mixtures with AA. In this case, overall basicity of the solvent decreased due to excess equivalent of AA in the solvent composition and solvent introduced limited DHF of PVDF and brown coloured solid obtained. In case of solvent with a mole ratio of 3:1, no peak for F atom was observed as the solvent possessed negligible basicity and indicated the lack of PVDF. Hence, solvents with alkaline characteristics allowed for the degradation of PVDF via the DHF process, and it was observed that amounts of individual components in the solvents influenced both the degradation ability as well as the physical appearances of the materials obtained after the process. Further, the IL and AA mixtures with AA:IL mole ratios more than 2:1 merely performed as a solvent where only dissolution of PVDF occurred without its decomposition.

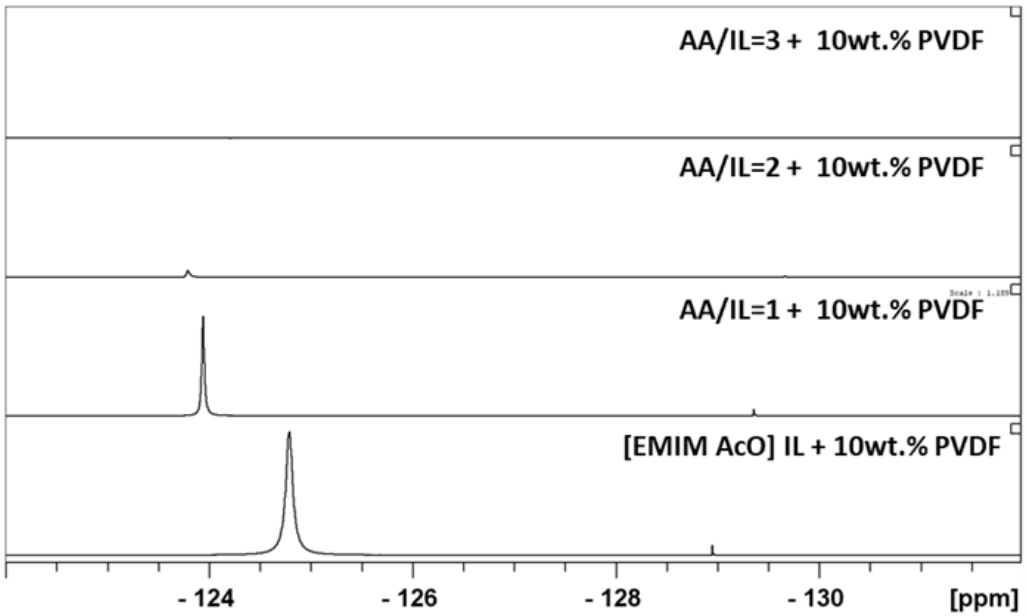

Figure 6. ^{19}F NMR of the reaction mixture after the thermal treatment of PVDF in pure [EMIM][AcO] IL and DESs with varying AA/IL mole ratios 1:1, 2:2 and 3:1.

3.6. ATR-FTIR Analysis of Treated PVDF

ATR-FTIR analysis of PVDF samples was performed to get insights for possible unsaturation induced by the DHF process as well as crystalline phase changes after thermal treatment in various solvents. As shown in Figure 7A, the broad peak in the range of 1490–1716 cm^{-1} for the conjugate and non-conjugated alkenes (-C=C- bond) was observed for the pure IL treated sample [40]. The sample obtained after the treatment in solvent with an AA:IL mole ratio of 1:1 also showed broad but lower intensity peak for -C=C- bond in the similar spectral range. However, a similar peak did not appear in case of

other samples processed in solvents with higher AA:IL mole ratios as well as pure AA. This observation is in correlation with ^{19}F NMR analysis of the reaction mixtures as well as physical appearance of the treated samples (Figures 4 and 6). The crystalline phase change from α to β is previously reported in PVDF under thermal treatment in various diprotic solvents [9,19]. Similar possible crystalline phase transition in the thermally treated PVDF materials with various solvents was also examined. The neat PVDF material gave rise to the characteristic absorption peaks for α-phase at 610, 761, 795 and 976 cm^{-1} and for β phase at 510, 840 and 1279 cm^{-1} [9]. Hence, it represents that the neat PVDF is composed of both α and β crystalline phases in its structure. For pure IL treated sample, the peaks at 1170 and 1382 attributed to symmetrical starching of -CF_2 and -CH_2 groups, respectively, were retained while the characteristics peaks corresponding to both α and β phase were disappeared. Further, the peaks for mixed crystalline phase were prominently visible for the sample treated in solvent with an AA:IL mole ratio of 1:1. It has been previously described that a sample treated in a solvent with an AA:IL mole ratio of 1:1 was not fully dissolved and a part of the solid remained unreacted. In case of thermally treated samples in solvents with AA:IL mole ratios of 2:1 and 4:1, the peaks assigned for the α phase disappeared whereas intense peaks correspond to only β phase were observed. This indicates that solvents capable for complete dissolution of PVDF during the process, facilitate the crystalline phase transition and the mixed phase comprised PVDF was converted to β phase rich material. On the other hand, the thermal treatment of PVDF in pure AA results in the formation of pure α phase rich material, since FTIR analysis represents that the peak corresponds to β phase disappeared and intense peaks attributed to the α phase were observed. The previous reports regarding the polarity dependent dissolution and phase transition described that the high dipole moment or polarity solvents such as DMSO, DMF, NMP and DMA were able to dissolve PVDF and to form a single phase, allowing for the α to β crystalline phase transition. On other hand, the medium to lower polarity and ketone functionality comprised solvents tend to have weaker solvent-polymer interaction and form α phase rich containing non-transparent thermochemical gel after thermal treatment [22]. The Kamlet-Taft parameters measurements in this report also provided a similar observation regarding the polarity of the applied solvents where IL and AA containing solvents possess higher polarizing ability compared to pure AA (Table 1). Hence, the applied solvents for the processing of PVDF are able to induce unsaturation and crystalline phase transformation due to their basicity as well as polarizing ability.

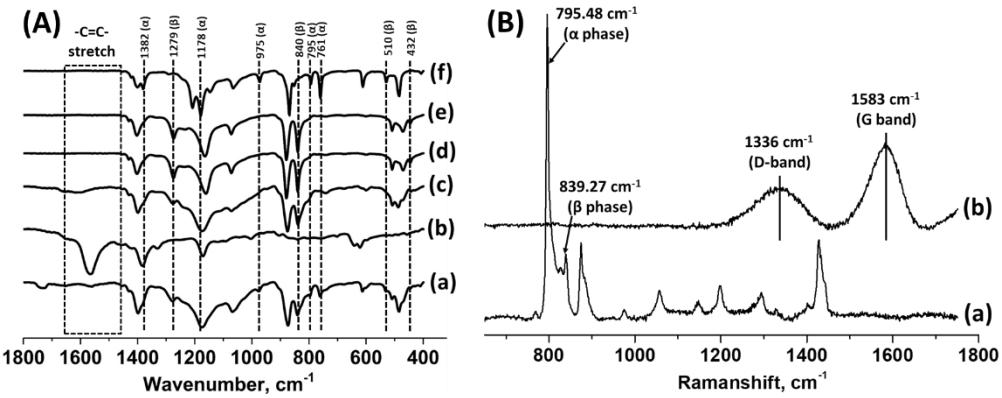

Figure 7. (**A**) ATR-FTIR spectra of neat PVDF and thermally treated PVDF in pure [EMIM][AcO] IL, AA and their mixtures with varying AA/IL mole ratios, (a) neat PVDF, thermally treated PVDF in (b) pure IL, (c) AA:IL = 1:1, (d) AA:IL = 2:1, (e) AA:IL = 4:1 and, (f) pure AA. (**B**) Raman spectra of (a) neat PVDF and, (b) thermally treated PVDF in pure [EMIM][AcO] IL.

3.7. Raman Analysis of Treated PVDF

Raman spectra recorded for neat PVDF and pure IL treated PVDF sample can be found in Figure 7B. Due to the fluorescence interference during analysis, instead of desired Raman

spectra, strong fluorescence signals with noise were observed for the samples obtained after treatment with IL and AA containing solvents and pure AA. Therefore, corresponding spectra are not represented. As shown in Figure 7(Ba), the peaks for CH_2 group in the α and β crystalline phases were observed at 795.48 and 839.27 cm^{-1}, respectively, for neat PVDF material which is analogous to FTIR analysis [41]. Surprisingly, in the case of pure IL treated samples, the peaks for the pure or dehydroflurinated PVDF (1522 cm^{-1} for -C=C- bond) were not present. On the other hand, peaks at 1583 and 1336 cm^{-1}, characteristic for G and D bands, respectively, in highly carbon rich material such as graphene, graphene oxide or activated carbon were observed. The G and D bands in carbon rich materials attributed to the out-of-plane breathing mode of the sp^2 carbon atoms associated with isolated double bonds (-C=C-) and defects in the structure, respectively [42]. Raman spectroscopy is usually employed for the analysis of above-mentioned carbonaceous materials in terms of structural defects by measuring the intensity ratio of D and G band, i.e., I_D/I_G. Since the intensity of the D band is lower than the G band, it represents that the sample obtained after treatment with IL had more isolated -C=C- bonds and the number of defects in the structure are low. Hence, similar to FTIR measurements, the Raman study also depicted that an extensive DHF of PVDF occurred in pure IL which further results in the formation of carbonaceous material.

3.8. ^{13}C MAS NMR Analysis of Treated PVDF

The ^{13}C MAS NMR analysis of the PVDF samples obtained after the treatment in pure IL and AA, as well as solvents obtained after their combinations was performed. As shown in Figure 8, neat PVDF showed peaks for CH_2 (44 ppm) and CF_2 (121.3 ppm) functional groups in its polymeric chains [43]. For pure IL treated PVDF, besides the less intense peaks for CH_2 and CF_2 groups, new broad peaks in between 95–120, 130–145 and 150–170 ppm were observed for various aromatic functionalities such as protonated aromatic, substituted aromatic and phenolic carbon atom, respectively [44]. Hence, analogous to the results obtained with FTIR and Raman analysis, solid-state NMR analysis also shows that pure IL induces the carbonization of PVDF through DHF process and forms sp^2 carbon atom rich cyclic aromatic functional groups in its structure. In case of IL and AA combined solvents with an AA:IL mole ratio of 1:1, 2:1 and 4:1 well as pure AA treated materials, no significant changes have been observed in NMR spectra, except peak broadening compared to neat PVDF.

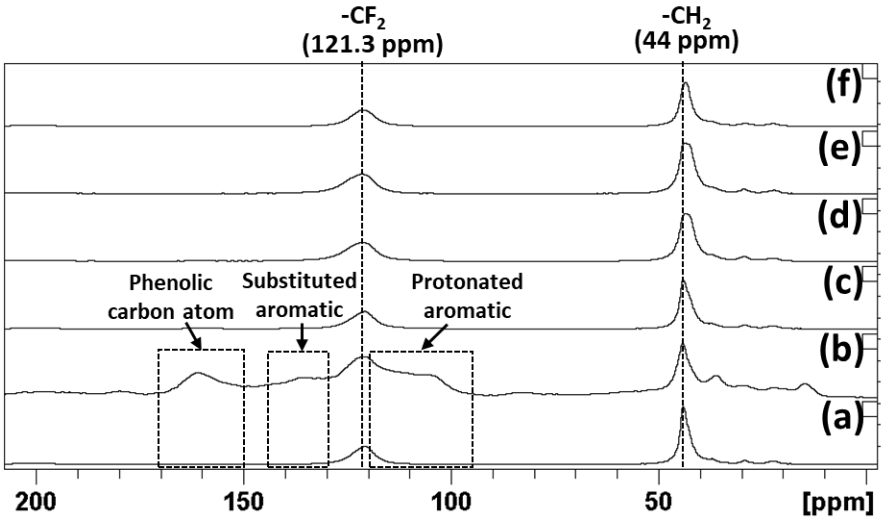

Figure 8. ^{13}C MAS NMR analysis of neat PVDF and thermally treated PVDF in pure [EMIM][AcO] IL, AA and DESs with varying AA:IL mole ratios, (a) neat PVDF, thermally treated PVDF in (b) pure IL, (c) AA:IL = 1:1, (d) AA:IL = 2:1, (e) AA:IL = 4:1 and, (f) pure AA.

Hence, various measurements including ^{1}H NMR analysis of IL and AA combined solvents, ^{19}F NMR analysis of the reaction mixture after PVDF thermal processing, FTIR, Raman, solid-state ^{13}C MAS NMR analysis of the treated PVDF represents that the pure and highly alkaline IL has introduced the significant changes in PVDF through DHF process and benzene ring comprised activated carbon and graphene oxide like material was obtained. These analyses also showed that the rate of PVDF degradation is steadily reduced when solvents containing IL and AA were applied.

3.9. XRD Analysis of Treated PVDF

The phase transitions in mixed phase PVDF after the thermal treatment in various solvents was further confirmed by XRD analysis and the obtained spectra are shown in Figure 9. The neat PVDF shows the characteristics diffraction peaks for the α phase at 18.16°, 18.79°, 20.31° and 26.95°, respectively, corresponding to the crystal planes such as (100), (020), (110) and (021), respectively. Identical to Raman and FTIR analysis, the XRD analysis also shows that the mixed phase PVDF is dominant in the α phase compared to the β phase in its composition and, the peaks obtained for the neat PVDF in XRD spectra are not identical to the pure α phase containing material [41]. After the interaction of neat PVDF in a solvent with an AA:IL mole ratio 2:1, the mixed phase material was transformed to the pure β phase since the peaks for the α phase disappeared while the characteristic peak for the β phase, at 20.90°, suggesting the crystal pane (200) appeared. Similar transformation was also observed for the samples treated in solvents with AA:IL mole ratios of 4:1 and 6:1. The pure AA treated PVDF sample gave rise to intense peaks belonging to pure α phase at 17.58°, 18.21°, 19.77 and 26.47°, respectively, for the previously mentioned crystal planes [41]. Further, it was also observed that the 2θ value of the characteristic peak for the β phase slowly decreased from 20.90° for the sample treated in the solvent with an AA:IL mole ratio of 2:1 to 20.76° and 20.58°, for the samples treated in the solvents with AA:IL mole ratios of 4:1 and 6:1, respectively. This suggests that as the AA amount increased in the solvent's composition, the crystalline phase transition of the mixed phase neat to pure α phase containing material steadily increased. Hence, as observed previously in the FTIR analysis, the XRD analysis also represented identical information regarding the crystalline phase changes for mixed phase PVDF in IL and AA combined solvents as well as pure AA. Considering these observations based on FTIR and XRD analysis, the selective crystalline phase transition in mixed phase PVDF can be achieved through the selection of either IL and AA comprised solvents or pure AA.

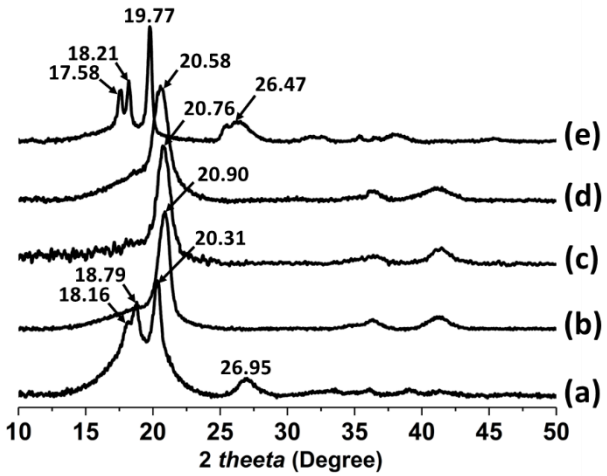

Figure 9. XRD analysis of (a) neat PVDF, thermally treated PVDF in DES, (b) AA:IL = 2:1, (c) AA:IL = 4:1, (d) AA:IL = 6:1 and (e) pure AA.

3.10. N_2 Physisorption Analysis of Treated PVDF

The N_2 physisorption analysis study of thermally treated PVDF samples in IL and AA containing solvents, and pure AA, were also performed to estimate their porous characteristics. Figure 10A,B show the N_2 absorption/desorption isotherms as well as BJH (Barret–Joyner–Halenda) desorption pore size distribution curves obtained after the N_2 physisorption study of these thermally treated PVDF samples.

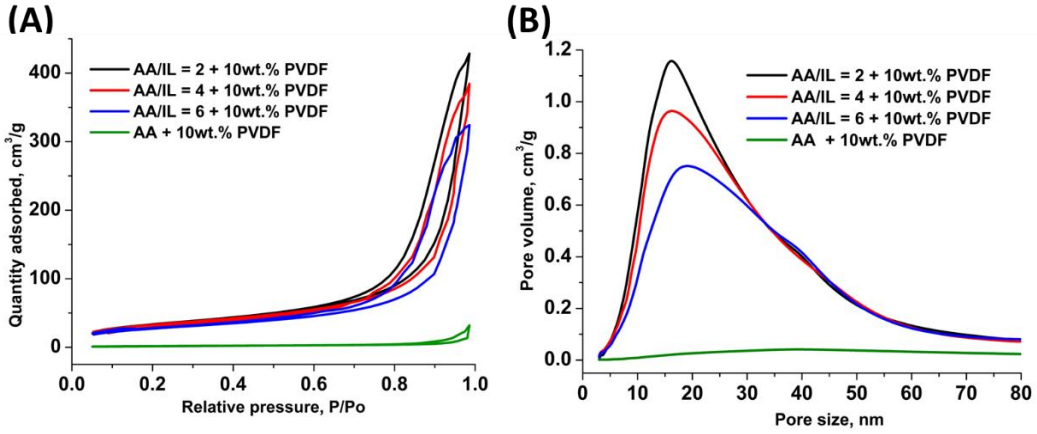

Figure 10. (**A**) N_2 absorption/desorption isotherms and, (**B**) BJH (Barret–Joyner–Halenda) desorption pore size distribution of thermally treated PVDF in DES with AA/IL = 2:1, 4:1, 6:1 or pure AA. Surface area (SA) for each sample is shown in the parenthesis.

As shown in Figure 10A, the samples obtained after the treatment with IL and AA combined solvents as well as pure AA gave rise to capillary condensation hysteresis loop with type IV adsorption isotherms (IUPAC classification) which is characteristics of mesoporous solids. In addition, it was also observed that with an increase in the AA:IL mole ratio from 2:1 to 6:1 in the composition of solvents, the amount of adsorbed N_2 was steadily decreased. Similarly, the surface area (SA) of the treated samples is decreased from 123 m^2/g for solvents with AA:IL mole ratio of 2:1 to 111 and 100 m^2/g for solvents with an AA:IL mole ratio of 4:1 and 6:1, respectively (Table 2). Further, Figure 10B shows that the wide pore size distribution with multi-scale pores (3–80 nm) were observed for treated PVDF samples where maxima of the pore distribution curves in the range between 16–20 nm was obtained. The BJH desorption average pore size as well as pore volume values were not significantly influenced in case of sample obtained after treatment in these solvents (Table 2). However, the decrease in the SA as well as area under the pore distribution curve with widening of pore size distribution indicates that the mesoporous characteristics are steadily decreased as the amount of AA in the solvent's composition increased. The samples treated in pure AA, showed that very low amount of N_2 got adsorbed even at high pressure region (P/Po = 0.98) and non-porous material obtained with significantly low SA (7 m^2/g) as well as pore volume (0.05 cm^3/g) compared to IL and AA combined solvents treated PVDF. The high pore size in case of pure AA treated sample could be result of interparticle distance or voids present in the particles. Hence, N_2 physisorption study shows that the besides the formation of β phase rich material, the porous characteristics can be also introduced in PVDF after its processing in IL and AA containing solvents.

Table 2. Surface area, pore size and pore volume of the PVDF samples obtained after treatment with various solvents.

Solvent	BET Surface Area (m^2/g)	Pore Size (nm)	Pore Volume (cm^3/g)
AA/[EMIM][AcO] = 2:1	123	16.01	0.66
AA/[EMIM][AcO] = 4:1	111	18.17	0.64
AA/[EMIM][AcO] = 6:1	100	21.52	0.61
Acetic acid (AA)	6.68	27.40	0.05

Porous characteristics measurement study shows that the porosity of the IL and AA containing solvents treated samples proportional to the amount of IL in solvents composition. As described previously, due to the DHF process in pure IL, the PVDF was extensively carbonised and graphene or activated carbon structures were formed. Pezzotti et.al. reported previously that thermal decomposition of PVDF in KOH to activated carbon due to extensive DHF process through the formation of the sp^2 carbon containing ring like structures [45]. The author also reported possible mechanism for the degradation of PVDF in alkaline condition and it can be applied to the present study of PVDF treatment in basic IL containing solvents (Figure 11). In pure IL, the PVDF initially converted to cis- and trans- form of unsaturated PVDF compounds (reaction 1) by DHF process and trans-forms were converted to -C=C- bond containing ring structures through continuous loss of HF (reaction 2). These ring structures showed their characteristics peaks in FTIR, ^{13}C MAS NMR and Raman analysis and confirmed formation of carbon rich materials. However, in case of IL and AA combined solvents, IL is less available due to its neutralisation and dilution by AA therefore it is possible that the controlled DHF process probably preceded in the PVDF polymer chains through cross-linking of PVDF (Figure 11, reaction 3). The cross-linking of the polymer chains likely introduced porous characteristics in the IL and AA combined solvents treated samples. Nevertheless, solvents with an AA:IL mole ratio of more than 2:1 results in excess equivalents of AA in their compositions and the rate of DHF process decreased which also reduced the cross-linking as well as the porosity in the treated samples. The pure AA barely allowed the dissolution of PVDF, as well as not being able to introduce the porosity in the treated material as the DHF process did not occur.

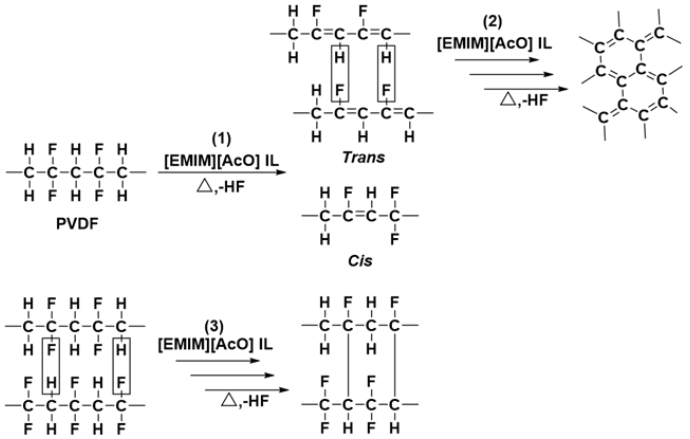

Figure 11. Schematics for the plausible mechanism for the (**1**) Dehydrofluorination (DHF), (**2**) Extensive dehydrofluorination (DHF) to sp^2 ring structures in PVDF in [EMIM][AcO] IL and (**3**) Cross-linking of the carbon chains in IL and AA combined solvents.

3.11. Size Exclusion Chromatography (SEC) Analysis of Treated PVDF

SEC analysis of the samples obtained after thermal processing in IL and AA combined solvents and pure AA was carried out to examine changes in the molecular weight distributions in their structures. The SEC chromatograms (RI detector response versus elution time) of neat as well as treated PVDF materials are shown in Figure 12 and corresponding M_n,

and M_w values and M_w/M_n ratio are summarized in Table 3. Neat PVDF showed single elution curve with an M_w of 209,123 g/mol, M_n of 45,983 and PDI of 4.55. In case of sample treated in solvent with AA/IL mole ratio 2:1, the M_n and M_w values increased while PDI value reduced to 2.61. Besides that, the broadened elution curve with less intensity was obtained for neat PVDF was further whereas new broad elution curves for high molecular weights polymeric entities were observed before the elution volume reach to 17 mL. Since the M_n increased more compared to M_w, it is possible that high molecular weight polymeric units have formed in the polymeric chains due to combination of controlled DHF and crosslinking process between dehydroflurinated polymeric units, which eluted before the low molecular weight polymeric units corresponds to neat PVDF (Figures 11 and 12). The intensity of the elution curves attributed to high molecular weight units were steadily decreased whereas the elution curve that belongs to neat PVDF appeared again as the solvents with AA/IL mole ratios 4:1 and 6:1 were applied for the processing. The PDI values of the treated samples were also increased to 3.51 and 3.78 for the solvents with AA/IL mole ratios 4:1 and 6:1, respectively. As observed previously, the increase in AA amount in the solvent composition decrease the rate of DHF process and subsequent crosslinking in the polymeric chains of PVDF. In case of pure AA treated sample, single elution curve as well as the PDI value equivalent to neat PVDF were obtained. Hence, IL and AA containing solvent with an AA:IL mole ratio of 2:1 not only formed material with highest porosity amongst applied solvents but it also allows the formation of high molecular weight units in the treated polymeric chains of treated PVDF. However, as shown in Figure 10 and Table 3, similar to solvent with an AA:IL mole ratio of 2:1, the solvents with higher mole ratios were also able to introduce the porous characteristics in PVDF after the processing even though their polydispersity after treatment had not significantly changed.

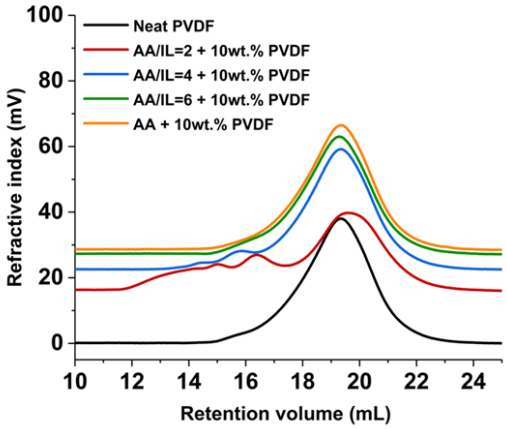

Figure 12. GPC chromatograms of the neat and treated PVDF samples in IL and AA combined solvents and AA.

Table 3. M_n, M_w and M_w:M_n ratio of neat PVDF and samples treated with IL and AA combined solvents and AA.

Solvent	M_n	M_w	M_w:M_n
Neat PVDF	45,983	209,123	4.55
AA/IL= 2:1 + PVDF	327,821	856,936	2.61
AA/IL= 4:1 + PVDF	62,931	220,316	3.51
AA/IL= 6:1 + PVDF	59,277	224,365	3.78
Acetic acid + PVDF	44,247	205,918	4.65

M_n = number average molecular weight, M_w = weight average molecular weight and M_w:M_n = polydispersity index, PDI.

3.12. Recovery of [EMIM][AcO] IL and AA Containing Mixture (AA:IL Mole Ratio of 3:1)

The reaction mixture comprised of solvent with an AA:IL mole ratio of 3:1 and dissolved PVDF was selected to show the recovery approach for the solvent after the thermal treatment. After separation of dissolved PVDF as well as extracting solvent acetone, the solvent was obtained with 93% recovery. In this case, low vacuum was applied during the separation of acetone from the mixture to avoid the loss of AA considering its volatility under vacuum. The current process for the recovery of solvent containing AA and IL was preceded with acetone considering its high volatility compared to AA. As shown in Figure 13a,b, the ^{1}H NMR spectra confirms that the solvent was recovered with high purity and no significant loss of AA was observed when comparing with the neat solvent.

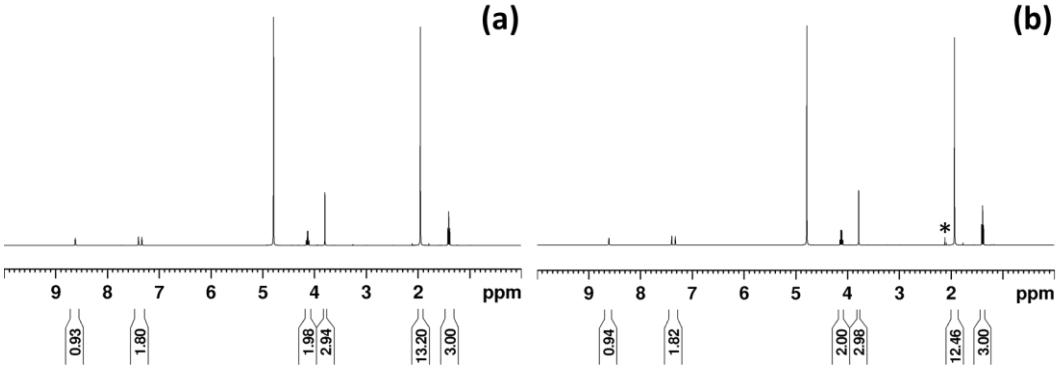

Figure 13. ^{1}H NMR spectra (in D_2O) of solvent with an AA:IL mole ratio of 3:1, (**a**) neat solvent and (**b**) recovered solvent (asterisk (*) shows acetone impurity).

4. Conclusions

The [EMIM][AcO] ionic liquid and acetic acid containing solvents were fruitfully applied for the thermal processing of PVDF where the physicochemical properties of the treated materials were varied based on the composition of the applied solvents. The DSC and Kamlet-Taft parameter study showed that the ionic liquid and acetic acid mixtures with various combinations were able to form polar low temperature transition solvents with varying basicity. FTIR and Raman as well as ^{13}C MAS NMR analysis showed that the highly basic as well as polar IL allowed the dissolution as well as extensive dehydroflurination of PVDF, resulting in highly carbonaceous material. The solvent composition with an equivalent mixture of an IL and acid having sufficient basicity and polarizability was not able to dissolve or dehydroflurinate PVDF effectively. The IL and acid mixtures with more than equivalent of AA possessed similar polar characteristics to IL and was able to dissolve PVDF with negligible or no dehydroflurination of PVDF. The FTIR and XRD analyses confirmed the transformation of neat and mixed phase PVDF to porous and β crystalline phase rich material, after the thermal treatment in IL and acid comprised solvents. Conversely, the treatment of neat PVDF in pure IL leads to the formation of an α crystalline phase containing material with non-porous characteristics. The SEC study showed that the polydispersity of PVDF decreased with an increase in the molecular weight after dehydroflurination and possible cross-linking in its polymeric chains, when a solvent with an AA:IL mole ratio of 2:1 was applied upon thermal treatment. The solvent comprised with AA to IL mole ratio of 3:1 was recovered with high purity and recovery after the thermal treatment of PVDF. Hence, the synthesis of industrially important electroactive β crystalline phase rich PVDF with desired porosity was achieved by thermal processing of PVDF in IL and acetic acid containing reversible solvent media. This thermal processing approach can be explored at industrial scale (e.g., PVDF recycle from lithium battery) since bulk availability of the IL is possible in near future (e.g., BASF, Solvionic, Scionix, etc.). Besides that, the process can be industrially economical since comparatively less amount of IL is required in the solvent composition compared to cheaper AA. The obtained electroactive phase rich PVDF material has the potential to be applied not only

in the electronic equipment, but considering porous characteristics, it can be also used to fabricate porous membranes for the separation techniques such as water purification and olefin-paraffin separation.

Author Contributions: S.G.K.: conceptualization, investigation, resources, visualization, validation, writing—original draft, project administration, writing—reviewing and editing; P.J.: resources, data curation, validation, formal analysis and writing—reviewing and editing; D.N.: resources, visualization, formal analysis and validation; V.M.D.: resources, visualization, formal analysis and validation; O.S.: resources, visualization, formal analysis and validation; K.I.: resources, visualization, data curation and writing—reviewing and editing; J.-P.M.: supervision, writing—reviewing and editing, data curation, validation, project administration and funding acquisition. All authors have read and agreed to the published version of the manuscript.

Funding: This work was funded by grants from the Swedish Research Council for Sustainable Development (project 2016-02011), part of the ERA-NET Marine Biotechnology framework.

Institutional Review Board Statement: Not applicable.

Informed Consent Statement: Not applicable.

Data Availability Statement: The data presented in this study are available on request from the corresponding author.

Acknowledgments: This work is part of activities of the Technical Chemistry, Department of Chemistry, Chemical-Biological Centre, Umeå University, Sweden. The Swedish Bio4Energy program and the Wallenberg Wood Science Center under auspices of Alice and Knut Wallenberg Foundation are gratefully acknowledged for funding part of this work. This work is also a part of the activities of the Johan Gadolin Process Chemistry Centre at Åbo Akademi University.

Conflicts of Interest: The authors declare no conflict of interest.

References

1. Ruan, L.; Yao, X.; Chang, Y.; Zhou, L.; Qin, G.; Zhang, X. Properties and applications of the β phase poly (vinylidene fluoride). *Polymers* **2018**, *10*, 228. [CrossRef]
2. Saxena, P.; Shukla, P. A comprehensive review on fundamental properties and applications of poly(vinylidene fuoride) (PVDF). *Adv. Compos. Hybrid Mater.* **2021**, *4*, 8–26. [CrossRef]
3. Wu, Y.; Li, Y.; Wang, Y.; Liu, Q.; Chen, Q.; Chen, M. Advances and prospects of PVDF based polymer electrolytes. *Chem. Eng. J.* **2022**, *64*, 62–84. [CrossRef]
4. Jain, A.; Prashanth, K.J.; Sharma, A.K.; Jain, A. Dielectric and piezoelectric properties of PVDF/PZT composites: A review. *Polym. Eng. Sci.* **2015**, *55*, 1589–1616. [CrossRef]
5. Sukumaran, S.; Chatbouri, S.; Rouxel, D.; Tisserand, E.; Zineb, T.B. Recent advances in flexible PVDF based piezoelectric polymer devices for energy harvesting applications. *J. Intell. Mater. Syst. Struct.* **2021**, *32*, 746–780. [CrossRef]
6. Kang, G.D.; Cao, Y.M. Application and modification of poly (vinylidene fluoride) (PVDF) membranes—A review. *J. Membr. Sci.* **2014**, *463*, 145–165. [CrossRef]
7. Grasso, G.; Galiano, F.; Yoo, M.J.; Mancuso, R.; Park, H.B.; Gabriele, B.; Figoli, A.; Driol, E. Development of graphene-PVDF composite membranes for membrane distillation. *J. Membr. Sci.* **2020**, *604*, 118017–118028. [CrossRef]
8. Jiang, B.; Zhou, J.; Xu, M.; Dou, H.; Zhang, H.; Yang, N.; Zhang, L. Multifunctional ternary deep eutectic solvent-based membranes for the cost-effective ethylene/ethane separation. *J. Membr. Sci.* **2020**, *610*, 118243–118252. [CrossRef]
9. Li, X.; Wang, Y.; He, T.; Hu, Q.; Yang, Y. Preparation of PVDF flexible piezoelectric film with high β-phase content by matching solvent dipole moment and crystallization temperature. *J. Mater. Sci. Mater. Electron.* **2019**, *30*, 20174–20180. [CrossRef]
10. Martins, P.; Lopes, A.C.; Lanceros-Mendeza, S. Electroactive phases of poly(vinylidene fluoride): Determination, processing and applications. *Prog. Polym. Sci.* **2014**, *39*, 683–706. [CrossRef]
11. Singh, N.; Madhav, H.; Yadav, S.; Jaiswar, G. Impact of vanadium-, sulfur-, and dysprosium-doped zinc oxide nanoparticles on various properties of PVDF/functionalized-PMMA blend nanocomposites: Structural, optical, and morphological studies. *J. Appl. Polym. Sci.* **2019**, *136*, 47116–47128. [CrossRef]
12. Sultana, A.; Sadhukhan, P.; Alam, M.M.; Das, S.; Middya, T.R.; Mandal, D. Organo-Lead Halide Perovskite Induced Electroactive β-Phase in Porous PVDF films: An Excellent Material for Photoactive Piezoelectric energy Harvester and Photodetector. *ACS Appl. Mater. Interfaces* **2018**, *10*, 4121–4130. [CrossRef] [PubMed]
13. Yuan, M.; Wang, H.; Li, H.; Yuan, C.; Wang, T.; Yang, H. Deep Eutectic Solvent—A Novel Additive to Induce Gamma Crystallization and Alpha-to-Gamma Phase Transition of PVDF. *Macromol. Chem. Phys.* **2022**, *223*, 2100416–2100425. [CrossRef]

14. Xing, C.; Guan, J.; Li, Y.; Li, J. Effect of a room-temperature ionic liquid on the structure and properties of electrospun poly(vinylidene fluoride) nanofibers. *ACS Appl. Mater. Interfaces* **2014**, *6*, 4447–4457. [CrossRef]
15. Vazquez, F.I.; Raghibi, M.; Bouzina, A.; Timperman, L.; Bigarréb, J.; Anouti, M. Protic ionic liquids/poly(vinylidene fluoride) composite membranes for fuel cell application. *J. Energy Chem.* **2021**, *53*, 197–207. [CrossRef]
16. Gebrekrstos, A.; Muzata, T.S.; Ray, S.S. Nanoparticle-Enhanced β-Phase Formation in Electroactive PVDF Composites: A Review of Systems for Applications in Energy Harvesting, EMI Shielding, and Membrane Technology. *ACS Appl. Nano Mater.* **2022**, *5*, 7632–7651. [CrossRef]
17. Marshall, J.E.; Zhenova, A.; Roberts, S.; Petchey, T.; Zhu, P.; Dancer, C.E.J.; McElroy, C.R.; Kendrick, E.; Goodship, V. On the solubility and stability of polyvinylidene fluoride. *Polymers* **2021**, *13*, 1354. [CrossRef] [PubMed]
18. Diorazio, L.J.; Hose, D.R.J.; Adlington, N.K. Toward a more holistic framework for solvent selection. *Org. Process Res. Dev.* **2016**, *20*, 760–773. [CrossRef]
19. Low, Y.K.A.; Tan, L.Y.; Tan, L.P.; Boey, F.Y.C.; Ng, K.W. Increasing Solvent Polarity and Addition of Salts Promote β-Phase Poly(vinylidene fluoride) Formation. *J. Appl. Polym. Sci.* **2013**, *128*, 2902–2910. [CrossRef]
20. Marino, T.; Russo, F.; Figoli, A. The Formation of Polyvinylidene Fluoride Membranes with Tailored Properties via Vapour/Non-Solvent Induced Phase Separation. *Membranes* **2018**, *8*, 71. [CrossRef]
21. Nishiyama, T.; Sumihara, T.; Sato, E.; Horibe, H. Effect of solvents on the crystal formation of poly (vinylidene fluoride) film prepared by a spin-coating process. *Polym. J.* **2017**, *49*, 319–325. [CrossRef]
22. Okabe, M.; Wada, R.; Tazaki, M.; Homma, T. The flory−huggins interaction parameter and thermoreversible gelation of poly(vinylidene fluoride) in organic solvents. *Polym. J.* **2003**, *35*, 798–803. [CrossRef]
23. Mohamed, A.; Yousef, S. Green and sustainable membrane fabrication development. *Sustain. Technol. Green Econ.* **2021**, *1*, 14–23. [CrossRef]
24. Milescu, R.A. Applications of the novel bioderived solvent Cyrene™ in polymer chemistry. Ph.D. Thesis, University of York, Heslington, UK, 2021. Available online: https://etheses.whiterose.ac.uk/29846/1/Milescu_201057084.pdf (accessed on 16 December 2021).
25. Ravikumar, V.R.; Schröder, A.; Köhler, S.; Çetinel, F.A.; Schmitt, M.; Kondrakov, A.; Eberle, F.; Eichler-Haeske, J.O.; Klein, D.; Schmidt, H.B. γ-Valerolactone: An Alternative Solvent for Manufacturing of Lithium-Ion Battery Electrodes. *ACS Appl. Energy Mater.* **2021**, *4*, 696–703. [CrossRef]
26. Zhenova, A.S. Green Solvents for Polymer Applications. Ph.D. Thesis, University of York, Heslington, UK, 2019. Available online: https://etheses.whiterose.ac.uk/25264/1/Anna_Zhenova_Thesis_2019.pdf (accessed on 28 January 2020).
27. Lora, M.; Lim, J.S.; McHugh, M.A. Comparison of the Solubility of PVF and PVDF in Supercritical CH_2F_2 and CO_2 and in CO_2 with Acetone, Dimethyl Ether, and Ethanol. *J. Phys. Chem. B* **1999**, *103*, 2818–2822. [CrossRef]
28. Dinoia, T.P.; Conway, S.E.; Lim, J.S.; McHugh, M.A. Solubility of Vinylidene Fluoride Polymers in Supercritical CO_2 and Halogenated Solvents. *J. Polym. Sci. B Polym. Phys.* **2000**, *38*, 2832–2840. [CrossRef]
29. Ueki, T.; Watanabe, M. Polymers in ionic liquids: Dawn of neoteric solvents and innovative materials. *Bull. Chem. Soc. Jpn.* **2012**, *85*, 33–50. [CrossRef]
30. Ptak, S.; Zarski, A.; Kapusniak, J. The importance of ionic liquids in the modification of starch and processing of starch-based materials. *Materials* **2020**, *13*, 4479. [CrossRef]
31. Brandt, A.; Grasvik, J.; Hallett, J.P.; Welton, T. D deconstruction of lignocellulosic biomass with ionic liquids. *Green Chem.* **2013**, *15*, 550–583. [CrossRef]
32. Guyomard, L.A.; Buchtova, N.; Humbert, B.; Bideau, J.L. Ion segregation in an ionic liquid confined within chitosan based chemical ionogels. *Phys. Chem. Chem. Phys.* **2015**, *17*, 23947–23951. [CrossRef]
33. Jablonski, P.; Nikjoo, D.; Warna, J.; Irgum, K.; Mikkola, J.P.; Khokarale, S.G. Sustainable, highly selective, and metal-free thermal depolymerization of poly-(3- hydroxybutyrate) to crotonic acid in recoverable ionic liquids. *Green Chem.* **2022**, *24*, 4130–4139. [CrossRef]
34. Zhang, Q.; Vigier, K.D.O.; Royer, S.; Jerome, F. Deep eutectic solvents: Syntheses, properties and applications. *Chem. Soc. Rev.* **2012**, *41*, 7108–7146. [CrossRef] [PubMed]
35. Francisco, M.; Bruinhorst, A.; Kroon, M.C. New natural and renewable low transition temperature mixtures (LTTMs): Screening as solvents for lignocellulosic biomass processing. *Green Chem.* **2012**, *14*, 2153–2157. [CrossRef]
36. Taft, R.W.; Kamlet, M.J. The solvatochromic comparison method. 2. The α-scale of solvent hydrogen-bond donor (HBD) acidities. *J. Am. Chem. Soc.* **1976**, *98*, 2886–2894. [CrossRef]
37. Kamlet, M.J.; Abboud, J.L.; Taft, R.W. The solvatochromic comparison method. 6. The π^* scale of solvent polarities. *J. Am. Chem. Soc.* **1977**, *99*, 6027–6038. [CrossRef]
38. Zhang, S.; Qi, X.; Ma, X.; Lu, L.; Deng, Y. Hydroxyl Ionic Liquids: The Differentiating Effect of Hydroxyl on Polarity due to Ionic Hydrogen Bonds between Hydroxyl and Anions. *J. Phys. Chem. B* **2010**, *114*, 3912–3920. [CrossRef]
39. Lin, J.; Malakooti, M.H.; Sodano, H.A. Thermally Stable Poly(vinylidene fluoride) for High-Performance Printable Piezoelectric Devices. *ACS Appl. Mater. Interfaces* **2020**, *12*, 21871–21882. [CrossRef]
40. Sierke, J.; Ellis, A.V. Cross-linking of dehydrofluorinated PVDF membranes with thiol modified polyhedral oligomeric silsesquioxane (POSS) and pure water flux analysis. *J. Membr. Sci.* **2019**, *581*, 362–372. [CrossRef]

41. Chipara, D.; Kuncser, V.; Lozano, K.; Alcoutlabi, M.; Ibrahim, E.; Chipara, M. Spectroscopic investigations on PVDF-Fe2O3 nanocomposites. *J. Appl. Polym. Sci.* **2020**, *137*, 48907–48920. [CrossRef]
42. Wei, Z.; Pan, R.; Hou, Y.; Yang, Y.; Liu, Y. Graphene-supported Pd catalyst for highly selective hydrogenation of resorcinol to 1, 3-cyclohexanedione through giant π-conjugate interactions. *Sci. Rep.* **2015**, *5*, 15664–15672. [CrossRef]
43. Montina, T.; Wormald, P.; Hazendonk, P. ^{13}C Solid-State NMR of the Mobile Phase of Poly(vinylidene fluoride). *Macromolecules* **2012**, *45*, 6002–6007. [CrossRef]
44. Cheng, H.N.; Wartelle, L.H.; Klasson, K.T.; Edwards, J.C. Solid-state NMR and ESR studies of activated carbons produced from pecan shells. *Carbon* **2010**, *48*, 2455–2469. [CrossRef]
45. Zhu, W.; Okada, K.; Li, Z.; Zhu, J.; Marina, E.; Pezzotti, G. Effect of component content variation on composition and structure of activated carbon in PVDF:K_2CO_3. *Phys. Chem. Chem. Phys.* **2019**, *21*, 2382–2388. [CrossRef] [PubMed]